

UPGRADED SYMPLECTIC 3D BEAM TRACKING OF THE J-PARC 3 GEV RCS

M. J. Shirakata, H. Fujimori and Y. Irie, KEK, Tsukuba, Japan

Abstract

The J-PARC 3 GeV ring is a rapid cycling synchrotron which consists of the large bore magnets. The beam tracking with the 3D distributed magnetic fields is kept developing in order to investigate the beam injection process. In order to improve the tracking accuracy and to save the calculation time, the symplectic integrator with the fractal decomposition method has been introduced. The updated simulation results of the beam injection on the J-PARC 3 GeV RCS and the improved performance of ‘Generic-Solver’ are presented in this paper. The quadrupole fields are also treated as the 3D distributed magnetic fields because they interfere with the bump magnet fields. The remarkable features on the large bore magnet system in the ring accelerator are also discussed.

SYMPLECTIC INTEGRATOR

A beam injection of the J-PARC 3 GeV RCS has been investigated with TRACY-II simulator by solving an equation of motion with a Lorentz force by the Runge-Kutta integration method[1][2]. However, it doesn’t insure the symplecticity of the particle dynamics. A symplectic integrator has been introduced in order to conserve the total energy of system. In addition, it is convenient to include a space-charge force.

The relativistic single-particle Hamiltonian in the electromagnetic fields[3] is given by

$$H(\vec{q}, \vec{p}, t) = c\sqrt{(\vec{p} - e\vec{A})^2 + m_0^2 c^2} + e\phi \quad (1)$$

where a scalar potential ϕ corresponds to a space-charge force without an external electrical field. The magnetic field $B(x, y, z)$ is given by the 3D-vector set distributed on a lattice structure. The time step Δt is set to the 1/5 of the minimum time while a particle passes through a cell. Though the magnetic field is a function of the location, it can be approximated to a constant vector during the time step Δt . In addition, the γ doesn’t change its value in the magnetic field. In these conditions, the time-evolution operator of the magnetic field $\exp(\Delta t D_M)$ can be given by simple matrices. When the Hamiltonian H can be written in a sum of two terms as: $H = H_M + H_U$, the corresponding time-evolution operator can also be divided to two components, such as:

$$\exp(\Delta t D_H) = \exp(\Delta t (D_M + D_U)). \quad (2)$$

The exponential operator product can be decomposed by using the fractal decomposition method[4] given in Eq. 3

and Eq. 4.

$$\begin{aligned} \exp(t(A + B)) &= \prod_{i=1}^r \exp(a_i t A) \exp(b_i t B) \\ &\quad + O(t^{m+1}) \\ &= S_m(t) + O(t^{m+1}) \end{aligned} \quad (3)$$

$$\begin{aligned} S_{2m}(t) &= S_{2m-1}(t) \\ &= S_{2m-2}^2(p_m t) S_{2m-2}((1 - 4p_m)t) S_{2m-2}^2(p_m t) \end{aligned} \quad (4)$$

where $p_m = 1/(4 - 2^{m-1}\sqrt{4})$. Adopting $m = 2$, the 4-th order symplectic integrator with space-charge force is obtained. This integrator has been installed into the Generic-Solver which is a sub-program of TRACY-II.

MAGNETIC FIELDS OF THE 3 GEV RCS

The recent design of the beam-injection system of the 3 GeV RCS is shown in Fig. 1, which is installed in a straight section. Because the beam tracking by the GenericSolver is carried out using the Descartes coordinate system, the z axis is identical to the s axis in this section. Two bump systems are prepared. One is the shift bump system to form an orbit offset of $x = 90$ mm at the carbon stripping foil on the charge-exchange injection, and the other is the paint bump system for beam painting. The shift-bump system will be fully excited during the whole injection period. On the other hand, the paint bump has a time dependency in order to paint up the RCS beam emittance of 216π mm mrad with the LINAC beam of 6π mm mrad. The injection process continues for about 320 turns. The carbon stripping foil is placed between SB2 and SB3. The foil position is defined as the injection point.

Correction for the Bump Magnets

The shift-bump magnets SB1 to SB4 are connected in series in order to form a shift-bump orbit. They are the identical magnets, and are required to excite the same strength magnetic fields. The Bl values obtained from the 3D magnetic field data are listed in Table 1. The Bl value is an integration of the B_y field along the z -axis.

Table 1: Bl values of the shift bump magnets at the center position: $x = y = 0$. Design value = 0.17559 Tm

Name	Bl [Tm]	Name	Bl [Tm]
SB1	0.17373	SB2	0.17548
SB3	0.17551	SB4	0.17365

Due to fringe interference, the Bl balance in the four bump magnets is broken, which causes a closed-orbit distortion, as shown in Fig. 2. Especially, the effective Bl

3 GeV Injection Bump (ver. RCS_2.323) rev. 2004.3.15

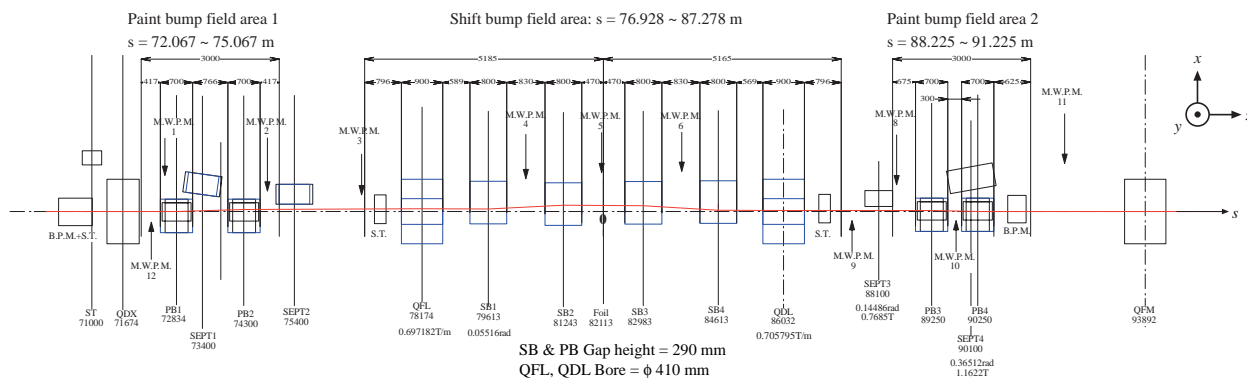


Figure 1: Layout of the beam-injection line of the J-PARC 3 GeV RCS.

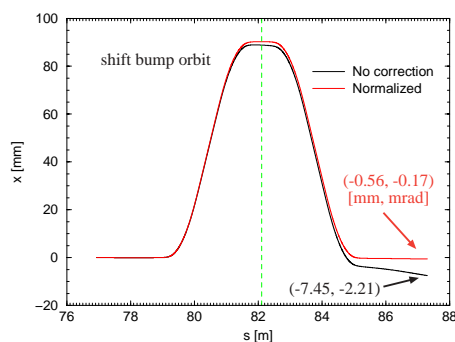


Figure 2: Central orbit trajectory in the shift bump area, which started from $x = y = 0$. The black line shows the COD, the red line is after the Bl correction, and the green dashed line indicates the stripping foil position ($s = 82.113$ m).

Table 2: Bump-orbit qualities with the shift-bump and paint-bump magnet fields at the injection point ($s = 82.113$ m).

	x (design) [mm]	x' (design) [mrad]
shift	90.26 (90.00)	-0.05 (0.00)
paint	41.09 (41.00)	-5.51 (-5.50)
all	131.44 (131.00)	-5.51 (-5.50)

values of SB1 and SB4 are about 1% smaller because the field tail becomes short, since the magnetic flux is diverted due to the existence of the quadrupole magnet core. The Bl correction is required in order to cancel the Bl unbalance, which is a mechanical adjustment on the actual magnets. In a calculation, the amounts of the magnetic fields were normalized by using the design Bl value in the GenericSolver program. The red line in Fig. 2 shows the bump orbit after Bl normalization. The residual COD can be suppressed. Similarly, the paint bump magnet fields are also corrected. The resulting bump orbit quality is summarized in Table 2.

Correction for the Quadrupole Magnet

Similarly to the dipole fields, quadrupole fields also deviate from the design value due to the field interference. In the case of quadrupole fields, the field deviation appears on a field gradient. The Gl value is defined as an integration of the field gradient along the z -axis. The focusing gradient deviation mainly causes the horizontal tune shift, and the defocusing gradient deviation mainly causes the vertical tune shift. A deviation of the field gradient is sometimes more harmful than the dipole field deviation. The field gradient was corrected by using the designed Gl values. Fig. 3 shows the reference particle motions in phase space. In order to see the trajectory, the particle positions for every turn are joined by linear lines. There is no tune difference with respect to the field-mesh size along the z -axis. The betatron tune shift, which corresponds to an amount of about 1% of field gradient, is observed in vertical phase space, compared to the design matrix, even after field gradient normalization. The origin of this deviation, however, comes from the changes in the magnet effective length. The effective length of the large-bore magnet extends, and the drift spaces on both sides of the quadrupole magnet are shortened. In the QFL and QDL cases, the drift spaces were shortened by about 100 mm for each side, which changed the betatron tune. For a further calculation, the tune shift was corrected by adjusting the Gl parameter.

The fringe field extends the effective length of the magnets, and in the case of the quadrupoles a tune shift occurs. The tune shift might sometimes be harmful when it is sufficiently long.

TRACKING RESULTS

In the J-PARC, the linac beam is collimated to 4π mm mrad by the collimator at the linac-to-RCS transport line. The beam emittance at the primary foil, however, is estimated to be 6π mm mrad at most if the beam blowup occurred by the space charge force after the collimator. At the beam injection line, beam passes through several kinds of time-varying fields until it reaches the primary stripping

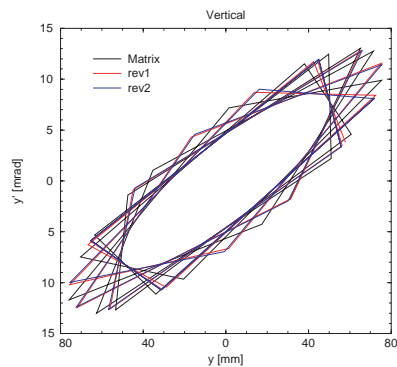


Figure 3: Particle trajectory in vertical phase space; rev1 corresponds to $\Delta z = 100$ mm mesh and rev2 corresponds to $\Delta z = 25$ mm mesh.

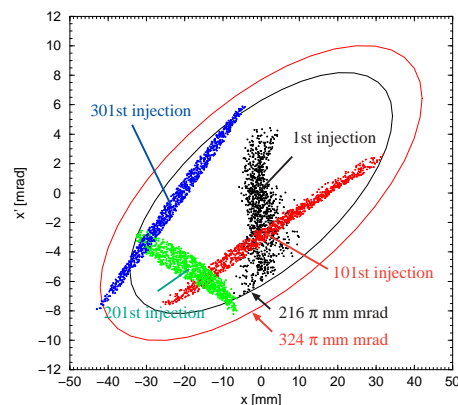


Figure 4: Phase-space distribution of the L3BT beam of 13π mm mrad in the horizontal plane at the injection point ($s = 82.113$ m) during 308 turns with painting the process. The 1st(black), 101st(red), 201st(green) and 301st(blue) injected bunches are traced.

foil such as the vertical painting magnets, the pulsed horizontal bending magnets which are utilized for changing the painting areas depending upon the beams for neutron users and the injection into the 50 GeV ring, the ring quadrupole magnet (QFL), and the shift bump magnets. The stabilities/precisions of these fields affect the effective emittance of the beam. Though the nominal emittance of the injection beam is defined as 6π mm mrad, the effective beam emittance, including the contributions of the stability of pulsed and AC power supplies, is estimated to be up to 13π mm mrad in the worst case. The phase-space distributions of the injected beams are shown in Fig. 4 and Fig. 5. The symplectic integrator represented the same result as the Runge-Kutta integration though the calculation speed was more than 5 times faster without space-charge contribution. Then, no remarkable difference was observed when the space-charge force of 8×10^{13} ppp was taken into account.

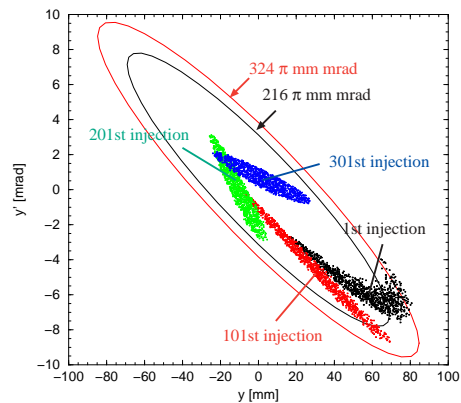


Figure 5: Phase-space distribution of the L3BT beam of 13π mm mrad in the vertical plane at the injection point ($s = 82.113$ m) during 308 turns with painting the process. The 1st(black), 101st(red), 201st(green) and 301st(blue) injected bunches are traced.

CONCLUSION

The 3D particle tracking simulation including the realistic fringe field is available by the TRACY-II simulator, which can take into account the 3D magnetic field distributions given by the magnet design code, TOSCA. The TRACY-II was applied to the design of the injection-straight section of the 3 GeV RCS of the J-PARC project, calculating the beam profile distribution of the painted beam. In this process, the followings can be noted:

- Introducing a symplectic integrator, the system phase volume is insured to be conserved.
- A symplectic integrator is more than 5 times faster compared to the Runge-Kutta integrator without space-charge contribution.
- Fractal decomposition method makes it easy to construct a symplectic integrator of an arbitrary order.
- There is no obvious difference in the tracking results of 3 GeV RCS injection process between two methods: Runge-Kutta integration and Symplectic integration.
- The effect from the space-charge force is not large with this simulation.
- Magnetic field interference between the closely located magnets breaks the field balance.
- A long fringe field of the large-aperture quadrupole magnets causes a betatron tune shift.

REFERENCES

- [1] M. Shirakata et al., Proceedings of EPAC2002, June, 2002 pp. 1670-1672.
- [2] M. Shirakata et al., Proceedings of SAST2003, November, 2003 pp. 389-391.
- [3] B. W. Montague, CERN 77-13, 19 July, 1977 pp. 37-51.
- [4] M. Suzuki, Phys. Lett. A Vol.146, num.6, 4 June, 1990 pp. 319-323.